Geopersia 2021, 11(1): 1-21
DOI: 10.22059/GEOPE.2020.295613.648523

RESEARCH PAPER

Integration of 3D seismic attributes and well logs for Asmari reservoir characterization in the Ramshir oilfield, the Dezful Embayment, SW Iran

Rahmat Sadeghi[1], Reza Moussavi–Harami[1,*], Ali kadkhodaie[2], Asadollah Mahboubi[1], Rahim kadkhodaie[3], Ahmad Ashtari[4]

[1] Department of Geology, Faculty of Sciences, Ferdowsi University of Mashhad, Iran
[2] Earth Science Department Faculty of Natural Science, University of Tabriz, Iran
[3] Research Institute of Petroleum Industries (RIPI), Tehran, Iran
[4] National Iranian South Oil Company (NISOC), Geophysics Department, Ahvaz, Iran

Received: 10 January 2020, Revised: 25 April 2020, Accepted: 02 June 2020

Abstract
3D seismic attributes and well logs were used to estimated porosity and water saturation in the Asmari Formation in the Dezful Embayment, SW Iran. For this purpose, at first, the 3D seismic volume was inverted base on the model, to obtain acoustic impedance cube. Afterward, the impedance and other attributes extracted from seismic volume were analyzed by multiple attribute regression transform and neural networks to predict porosity and water saturation between wells. Then linear or non–linear combinations of attributes performed for porosity and water saturation prediction. The result shows that the match between the actual and predicted porosity and water saturation improved; using only a single attribute to the derived multi attribute transforms and neural networks model. Based on the results of neural networks, the highest cross–correlation was observed between seismic attributes and the observed target logs between seven wells in the study area. Based on our study, the cross–correlation between actual and predicted porosity and water saturation increased and reached 93% and 90% respectively in the case of using probabilistic neural networks (PNN). Finally, according to the cross–validation results, PNN neural networks are used for porosity and water saturation prediction. We carry out porosity and water saturation slicing from the Asmari Formation for display lateral and vertical heterogeneities, and the result provided a reliable picture from subsurface formations. Porosity maps distribution shows the western portion of the structure is highly porous and should be considered for further exploration and development purposes. A possible reason for this high porosity in the western portion of the studied formation is the presence of sand layers, especially in zone 2.Note that sand volume increased towards west and northwest in direction of shadegan and Ahvaz fields and decreased towards east and southeast to Rag–e–Sefid field. Based on the result between acoustic impedance and core, changes in acoustic impedance were related to changes in the geological nature of the Asmari reservoir in the field. Accordingly, seismic inversion is a powerful tool for studying the details of lithology and sedimentary facies.

Keywords: Seismic Inversion, Multi–Attribute, Neural Network, Multiple Regression, Ramshir Oil Field, Asmari Reservoir.

Introduction

Porosity and water saturation distributions are crucial properties of hydrocarbon reservoirs and

* Corresponding author e-mail: moussavi@um.ac.ir

are involved in almost all calculations related to reservoir and production. Seismic inversion is a procedure that helps to extract underlying models of the physical characteristics of rocks and fluids. Usually, seismic and well–log data used to calculate physical properties. Evaluation of reservoir rock properties and mapping their internal heterogeneities are considered as primary steps in reservoir modeling. Data used in these cases include core, well log and well test data, production history and seismic studies (Rezaee, 2006). However, information obtained from cores and well logs are local and represent reservoir properties from a small portion of the reservoir (John et al., 2005). In heterogeneous reservoirs, lateral variations of reservoir property cannot be described from the measurements at separately located wells, because of the presence of high complication and heterogeneity. In order to overcome this problem, the integration of 3D seismic attributes and well logs are essential for creating various models of geology and reservoir properties between wells in the regions. (Abreu et al., 2003; Pramanik et al., 2004; Saltzer et al., 2005; Rezvandehy et al., 2011; Raeesi et al., 2012; Snedden, 2013; Perez–Munoz et al., 2013; Faraji et al., 2017; Aleardi, 2018). Seismic attributes are derivative quantities extracted from seismic data to obtain more information and are used in subsurface for interpretation of structures, stratigraphy, and lithology (Chen & Sidney, 1997). Nowadays, most of the research efforts to the inversion and interpretation of variations of seismic reflection data are dependent on the change in distance between source and receiver (AVO) from prestack data. However, post stack data still widely used because of their availability, low time–consuming and fast processing rates (Leite & Vidal, 2011). A number of methods are existing for seismic inversion. In this study, the model–based inversion was used to obtain the cube of full band acoustic impedance. Acoustic impedance (AI) Inversion produces high–resolution images of the subsurface leading to a significant enhancement in the interpretation of the seismic volume (Haris et al., 2017). The post stack acoustic impedance (AI) inversion methods became popular when algorithms of wavelet amplitude and phase spectra extraction became available (Lindseth, 1979). During the last decades, seismic attributes have successfully been used for different purposes in reservoir characterization (Kadkhodaie–Ilkhchi et al., 2009; Raeesi et al., 2012; Na'imi et al., 2014; Iturrarán –Viveros & Parra, 2014; Farfour et al., 2015) Seismic attributes extracted from 3D seismic data in combination with statistical methods (the multivariate regression and the probabilistic neural network (PNN) have been successfully employed to estimate reservoir properties prediction. likewise, several researchers focused on predicting porosity (e.g., Pramanik et al., 2004; Ogiesoba, 2010; Leite & Vidal, 2011; Khoshdel & Riahi, 2011; Kadkhodaie–Ilkhchi et al., 2014; Naeem et al., 2015; Maurya & Singh, 2019) and water saturation (Kadkhodaie–Ilkhchi et al., 2009; Na'imi et al., 2014) from various post stack seismic attributes by using multi–linear regression, neural network analysis, and fuzzy system. Based on the results, some seismic attributes were directly sensitive to the reservoir or specific lithological property. In the current study, water saturation and effective porosity were predicted from seismic attributes, along with seismic inversion by applying multi–attribute regression analysis and neural network in the Asmari reservoir, Ramshir oilfield. In addition, in order to reach sedimentary facies and its propagation in the reservoir, a correlation was established between seismic data and log data from 24 wells together with core from 7 wells, based on the seismic inversion results**.**

Geological setting of the study area

The Oligocene–Miocene shallow–marine carbonates of the Asmari Formation are the giant hydrocarbon reservoir at the margin of the Zagros Basin in southwestern Iran. This study focuses on mixed siliciclastic–carbonate deposits of the Asmari Formation in the Ramshir Oil Field, located in the Dezful Embayment, (Fig. 1).

The Dezful Embayment, situated in the south–central part of the Zagros fold–thrust belt, hosts

most of the onshore hydrocarbon reservoirs of Iran. It is bounded from the northeast by the Mountain Front Fault (MFF), from the north by Balarud Fault (BF), whereas in the east is limited by Kazerun Fault (KF) (Sepehr & Cosgrove, 2005). The studied field, Ramshir oilfield, is located about 80 Km south–east of Ahvaz (SW Iran) in the Dezful Embayment (Fig.1). Generally, the Asmari Formation conformably overlies the deeper facies of the Pabdeh Formation and the Gachsaran Formation unconformably overlies the Asmari Formation in most places. Lithologically, the Asmari Formation consists of thin, medium to thick and massive carbonate layers. Some sandstone layers (the Ahvaz Member) and anhydrite deposits (the Kalhur Member) are also present (Fig. 2).

Based on the petrographical studies and core description, the depositional system of the Asmari Formation changed from shallow marine to coastal plain in several times in the Ramshir oilfield. Such deposits indicate a low input of clastic sediment and mostly within arid settings. (Osleger et al., 1996). Asmari reservoir in the studied area was divided into 8 main zones and 7subzone based on geological and petrophysical characteristics (Table 1) which mainly include limestone, dolomite, and sandstone. Here, sandstones contain a majority of the hydrocarbons of the reservoir due to high porosity. Zone 1, in the upper part of the formation, underlies the cap rock (Gachsaran Formation), and Zone 8 (deepest zone) overlays shale and marls of the Pabdeh Formation. Zones 1, 6, 7 and 8 are mainly composed of limestone and dolomite, whereas zones 2, 3, 4 and subzone 5–2 have a variable amount of sandstone and shale. The highest volume of sandstone exists in subzones 2–1, 2–3 and 5–2.

In this reservoir, most of the production comes from zone 2, 1, 3 and 4 respectively which mainly consists of sandstone, dolomite, along with some interbeds of carbonate and shale. Other zones are saturated with water and are not productive zones (NISOC, 2016).

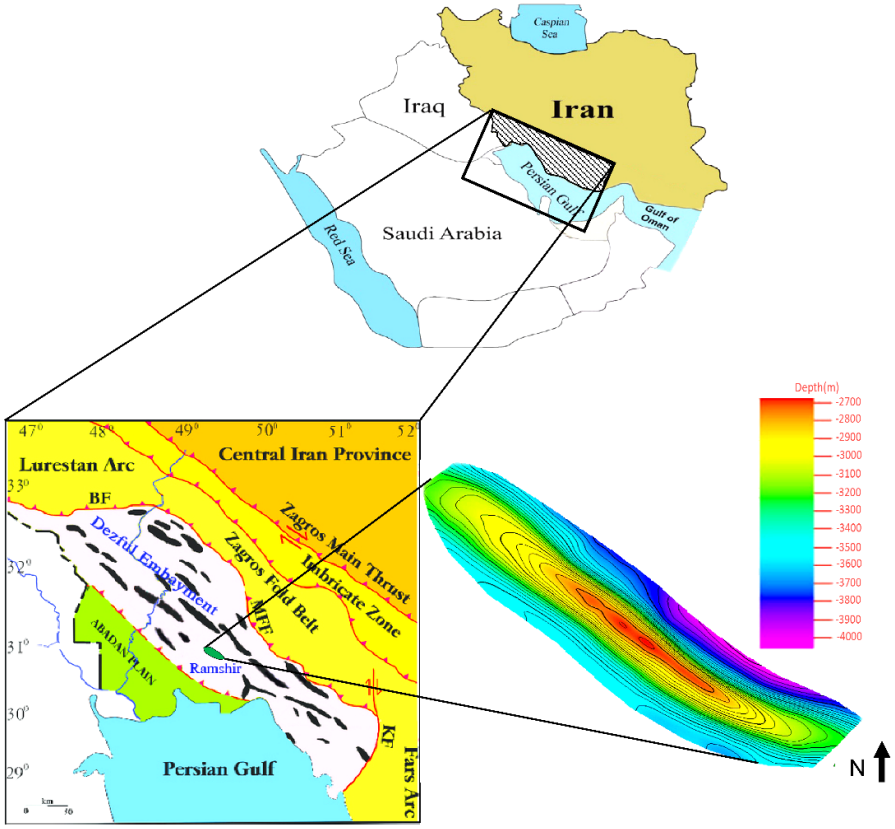

Figure 1. Location map of the Ramshir Field in southwestern Iran. The major late cretaceous and Tertiary oilfields in the region are also shown (Sepehr et al., 2005)

Table 1. Different reservoir zones/subzones of the Asmari Formation in the Ramshir oilfield

Asmari Reservoir Zonation: Summary of lithological and petrophysical average data								
Zones/ subzones	**Thickness (m)**	**(%)**	**Sw(%)**	**Lithology (%)**				
				LST.	**DOL.**	**SST.**	**SH.**	**ANHY.**
Z_1	36	12.35	40.40	30.30	49.40	0.00	2.30	0.00
S.Z_2.1	16	13.97	49.60	23.30	2.00	48.30	16.80	0.90
S.Z_2.2	5.3	14.06	33.05	30.50	44.00	5.70	4.80	0.00
S.Z_2.3	10.50	20.00	34.36	5.30	0.50	77.30	13.20	0.00
S.Z_3.1	21.86	8.20	63.53	43.50	25.70	0.50	6.50	0.00
S.Z_3.2	25.40	8.10	76.14	44.00	22.60	2.70	7.00	1.00
Z_4	28.10	9.70	84.85	30.00	14.00	14.20	16.60	0.20
S.Z_5.1	39.50	12.50	80.15	55.20	5.90	1.00	4.60	0.00
S.Z_5.2	24.50	14.83	87.02	22.90	3.30	50.50	17.60	0.00
Z_6	77.90	11.68	68.64	52.90	6.10	1.00	2.70	0.00
Z_7	71.40	8.90	56.85	63.40	10.20	0.00	1.20	0.00
Z_8	39.70	2.70	90.00	57.90	0.00	0.00	35.60	0.00
Total Avg.	396.16	11.42	63.72	38.27	15.31	16.77	10.74	0.18

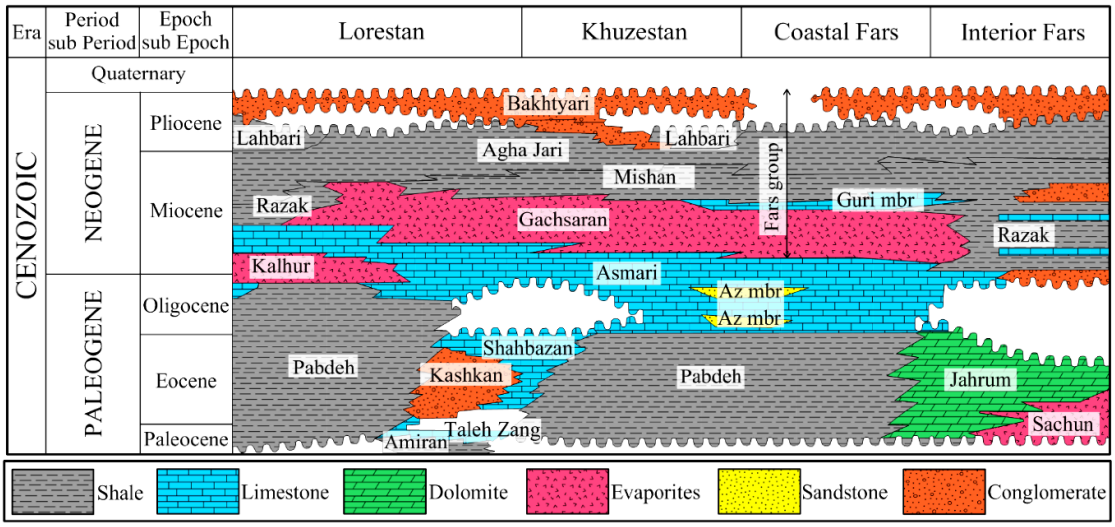

Figure 2. Schematic picture showing the relationship between the Cenozoic Formations, the Zagros Basin. Lateral change in thickness and lithology of the Asmari Formation in different parts of the basin is observed (Schlumberger, 2003)

Methodology

In this study, we used well log data including sonic (DT) and bulk density (RHOB) together with calculated logs including water saturation (SW) and effective porosity (PHIE) from seven cored wells of the Asmari reservoir of the Ramshir oilfield. The quality of data were controlled and ranked based on their validity. In this respect, corrections such as cable tension effects for adaptation of core and well log data readings, removal of bad hole flags (BHF) data, cycle skipping, removal of null values and log tails were performed.

To calculate the effective porosity correctly, shale volume was measured and the porosity of

the shale was removed from all computations. Seismic data used in this study are 3D processed and post stack seismic data from the Prospectiuni, S.A. & Pedex, survey (2009). At the next step, all data were loaded in Hampson–Russell Software (HRS10), and an integrated workflow was regarded. For this aim, a well–to–seismic tie was doing to pick out the key stratigraphic surfaces which were interpreted to create horizon maps. The created horizons maps, with the integration of necessary well log and post stack seismic data by seismic inversion method, resulted in the creation of the acoustic impedance cube in the studied field. The inversion procedure involves well to seismic calibration, wavelet estimation, low–frequency model estimation and model based inversion for a seismic dataset of Ramshir oilfield (Fig 3) (Huuse & Feary, 2005; Kumar et al., 2016). Afterward, effective porosity and water saturation were estimated from 3D post stack data in the HRS environment by using multi–attribute regression analysis and neural networks. Finally, the results were explained and interpreted based on the geological setting and diagenetic features of the Asmari reservoir in the field.

Seismic inversion

Seismic inversion is the integration of well log and seismic data by inverse modeling of the logs from the seismic data (Hampson et al., 2001).The common inversion method for invert seismic data and create a cube of full band acoustic impedance is named model–based inversion (Russell & Hampson, 1991). Model Based inversions are the generalized linear algorithm that uses an iterative forward modeling and comparison process (Simm & Bacon, 2014). The precision of seismic inversion results depends upon geologic characteristics, logging data, and seismic data resolution.

The inversion procedure of the seismic inversion for the 3D seismic cube of the Ramshir oilfield involves,

- Well to seismic calibration and wavelet extraction - Low–Frequency model generation
- Model based inversion (Lavergne & Willim, 1977; Lindseth, 1979; Hampson et al., 2001).

A well–to–seismic tie was created through a synthetic seismogram in order to identify two horizons of the Asmari and top of the Pabdeh Formations. Accordingly, these horizons were picked for use in the initial model building of the model based inversion. A brief review of the steps involved in performing seismic inversion is discussed as follows.

Well to seismic calibration and wavelet extraction

Theoretically, seismic inversion is based on the convolution model and states that the synthetic trace, can be generated from the coevolution of Earth's reflectivity series with the desired wavelet (Mallick, 1995; Cooke & Cant, 2010) such that:

$$S(t) = W(t) * R + N \quad \text{(Eq. 1)}$$

where is the extracted statistical wavelet, is the reflection coefficient (RC) series and is the random noise. at the first step of inversion, seismic and well logs data were imported to the inversion project, and well logs for each of the twenty–four wells were converted to a two–way travel time using check shot data. Then, the product of sonic and density logs provide an acoustic impedance log at each well place. This impedance log was used to derive a log of reflectivity. In the next step, the reflectivity was converted from depth to time by a suitable time–depth relationship, based on available check shot data for each of the well. The reflectivity was convolved with an appropriate wavelet to finally generate synthetic seismogram. The suitable statistical wavelet for each well was obtained by using the extraction and selection of various wavelets, which created the best correlation between synthetic and real traces. It is worth noting that a good correlation between synthetic traces derived from well logs and

original seismic traces at each well place comes from a good approximation of seismic wavelet (Kadkhodaie–Ilkhchi et al., 2013). After obtaining wavelet for each well and doing calibration procedure for each of the twenty–four wells, all calibrated wells were used together to obtain one average wavelet, which was used for the inversion. Figure 4 shows the extracted statistical wavelet from seismic data along with its amplitude and phase spectra. The dotted line displays the average phase of the wavelet. Figure 5 shows the picked time horizons of the Asamri and Pabdeh. The window length used in the wavelet extraction ranges from 1680 to 1840 ms, with a wavelength of 200 ms. The wavelet extraction algorithm uses seismic data and all available wells. A sample of a well–to seismic tie, for one of the wells in the Ramshir field, is shown in Fig. 6 where the correlation between synthetic seismogram (blue) and composite trace (red) at well location is 0.68%.

Low Frequency model

To generate low–frequency models, the input seismic data is modeled by hard constrained algorithms. This model is essential for seismic inversion especially model based inversion (Cooke & Schneider, 1983, Khoshdel & Riahi, 2007). In a model based inversion, low frequency data is usually generated by interpolation based on log data, horizon interpretation, and processing velocities. In this study, based on the interpolation of impedance logs from the twenty–four wells along with the interpreted seismic horizons (top of the Asmari and top of the Pabdeh formations). an arbitrary seismic line passing through the well locations is shown in Fig. 7.

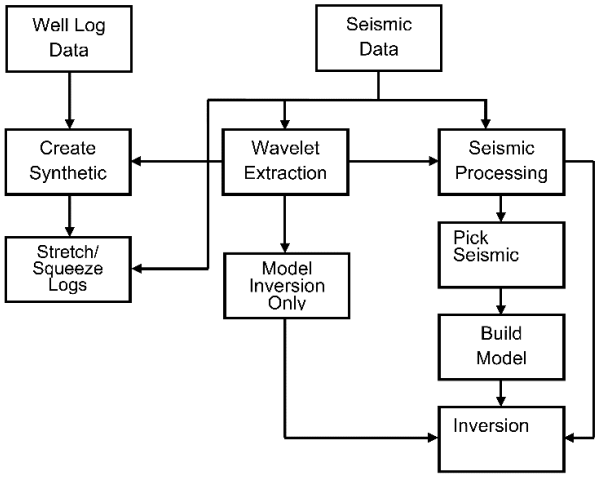

Figure 3. workflow for seismic post stack model-based inversion (Swisi, 2009)

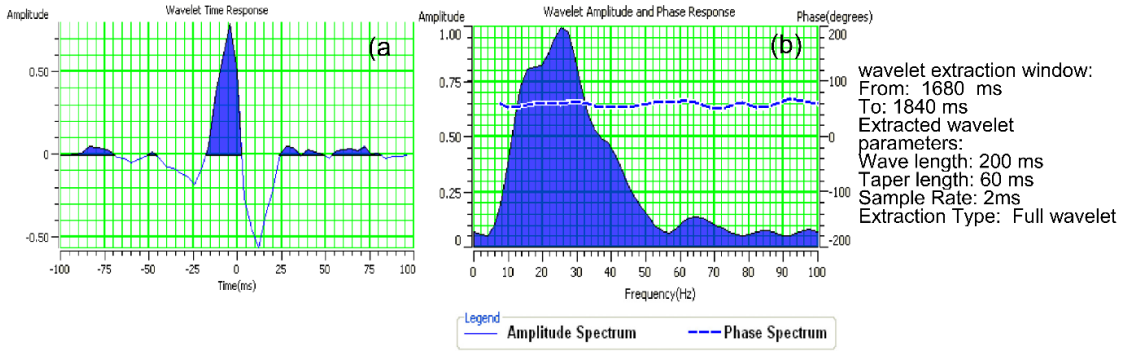

Figure 4. Average wavelet extracted, a) in a time domain and b) in the frequency domain

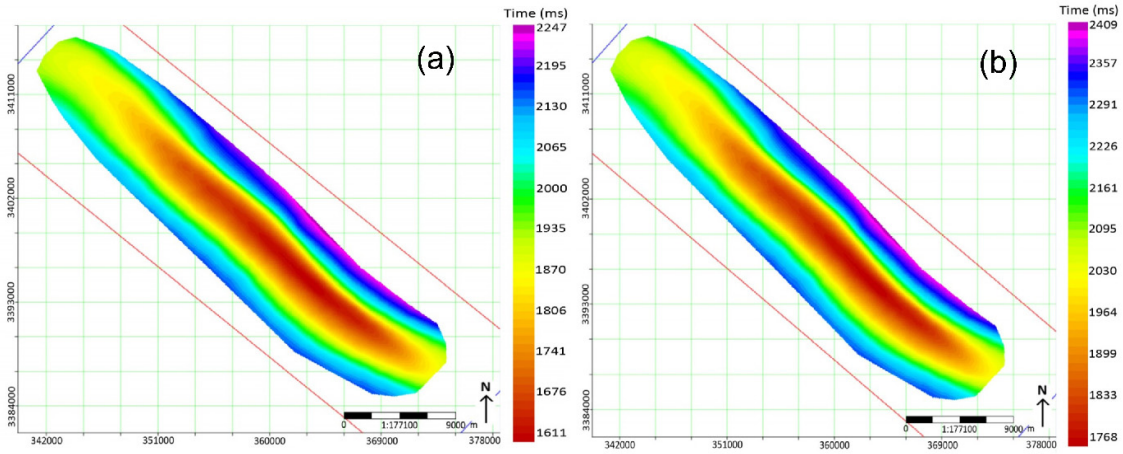

Figure 5. The time horizon of (a) Asmari Formation and(b) Pabdeh Formation

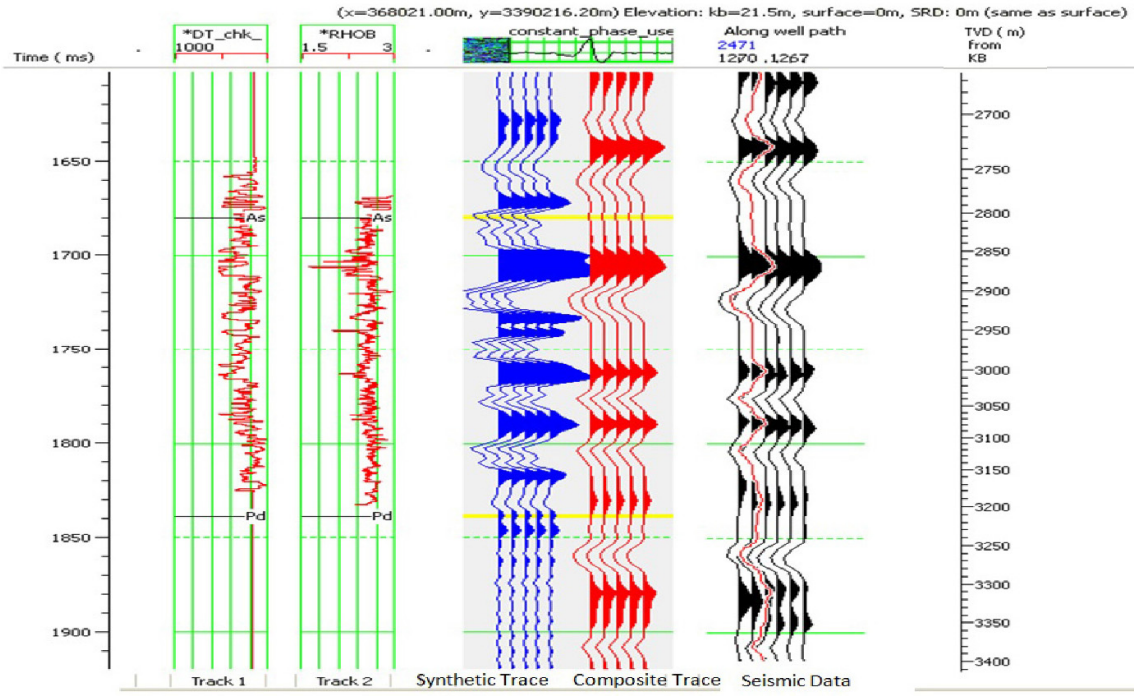

Figure 6. result of well to seismic tie for one of the wells in the Ramshir field showing the synthetic seismic generated from wavelet and well data (blue trace) and sampled seismic data close to the well (red) with a correlation coefficient of 68%

Model–based Inversion

A generalized linear inversion algorithm is used in model based inversions. This algorithm assumes that the seismic trace and the wavelet are known by the interpreters, and tries to alter the initial guess model until the calculated trace matches with the actual trace to an acceptable level (Russell, 2004).

In other words, the geological model is altered until the error between the synthetic and original seismic traces is minimized. The basic approach used in the inversion algorithm is, therefore, to solve the function given in Equation 2 and to measure any misfits between real and synthetic data (Russell, 2004)

$$J = Weight_1 \times (S - W * R) + Weight_2 \times (M - H * R) \quad \text{(Eq. 2)}$$

where S is the actual seismic trace, W is the extracted statistical wavelet, R is reflection co–efficient, M is the initial guess model or interpreted horizon data and H defines the integration operator, which is convolved with final reflectivity to produce the final impedance. In Equation 2, the first part models the seismic trace while the second part models the impedance initially estimated. Well data is used to control the small amounts of noise or modeling errors. The workflow for model based inversions is shown in Figure 3. The model based inversion technique is successful in capturing the lateral variations in acoustic impedances by incorporating spatially constant low frequency model (Figure 7). This inversion method was run with the appropriate wavelet and the background impedance model, resulting in an impedance model which needs to be closely compared with the actual impedance as a QC step. Figure 8 displays a final impedance section in one of the studied seismic arbitrary lines (violet color displays high AI reservoir intervals and green color indicates low AI intervals).

Porosity and water saturation estimation

Prediction of rock physical parameters such as porosity and water saturation is essential for the exploration and development of hydrocarbon reservoirs. In seismic reservoir characterization, porosity and water saturation are the main property which controlled hydrocarbon accumulation. These parameters affect the signature of the seismic data significantly. In this study, the acoustic impedance derived from seismic inversion associated with other suitable seismic attributes is used for the estimation of petrophysical parameters from well logs. There are a lot of combination of attributes that can be used to obtain a more reliable relationship between seismic attributes and reservoir properties such as neural networks, geostatistics, artificial intelligence and the genetic algorithm (Schultz et al., 1990 a,b; Yao & Journel, 2000; Chopra & Marfurt, 2007; Bosch et al., 2010; Raeesi et al., 2012; Perez–Muñoz et al., 2013; Snedden, 2013; Iturrarán–Viveros & Parra, 2014; Kadkhodaie–Ilkhchi et al., 2014).

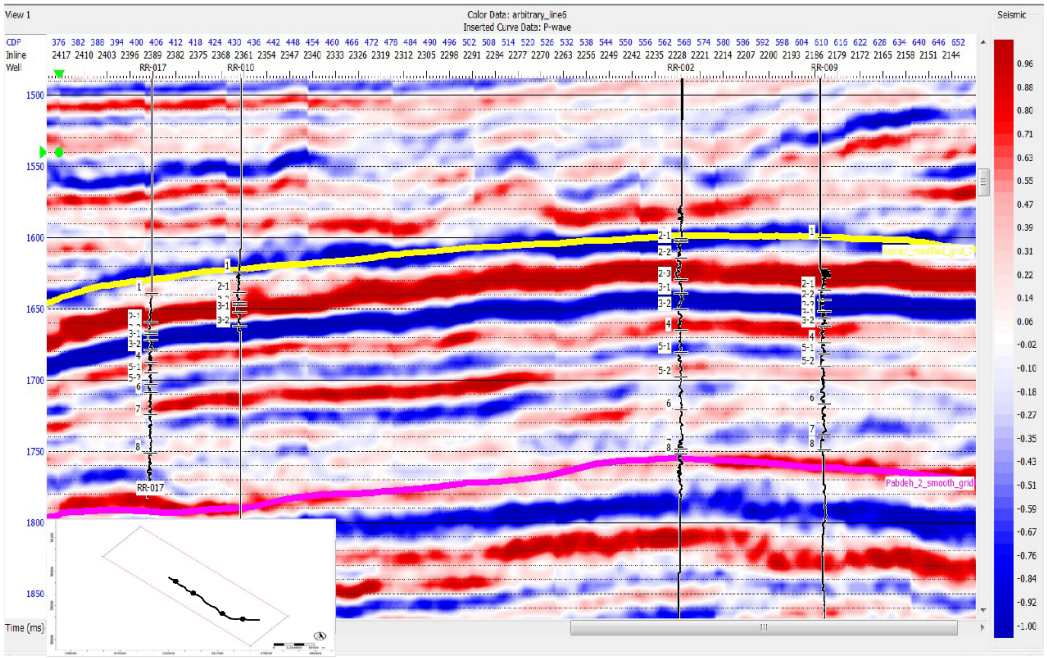

Figure 7. An arbitrary line from seismic data passing through four well locations. Yellow lines indicate top of Asmari Formation and violet color show top of Pabdeh Formation.

In this study to find a reliable relation between seismic attributes (as input data) and petrophysical parameters (as target data) single and multi–attribute regression analysis (with stepwise regression for selection of suitable attributes) and neural network algorithm were employed to predict effective porosity and water saturation.

Application of single attribute regression analysis for porosity and water saturation prediction

A linear regression technique is used to find the correlation coefficient between the target parameter with different seismic attributes. The results from a single attribute analysis are given in Table 2. The simplest method to create the relationship between the data and the seismic attribute is to use least squares method to determine the relationship. In this relation, high correlation regardless of its negative or positive value indicates a strong relationship between two parameters. According to Table 2, the prediction error is calculated for every attribute, and the one with the lowest error is the best single attribute.

The acoustic impedance from seismic inversion has the highest degree of correlation and the lowest degree of error related to porosity, otherwise, the Dominant Frequency attribute has the highest correlation with water saturation. In most cases that have dealt with seismic attributes, a single attribute is usually not enough to predict physical properties with a high degree of confidence (Tonn, 2002). Indeed, many attributes could be combined to derive the best relationship between seismic data as extracted attributes, thus, a multi–linear regression was used to estimate petrophysical property in the Asmari reservoir.

Application of multi–attribute regression analysis for porosity and water saturation prediction

A multi–regression analysis is a simple and useful method to find the strongest inputs for predicting a target parameter.

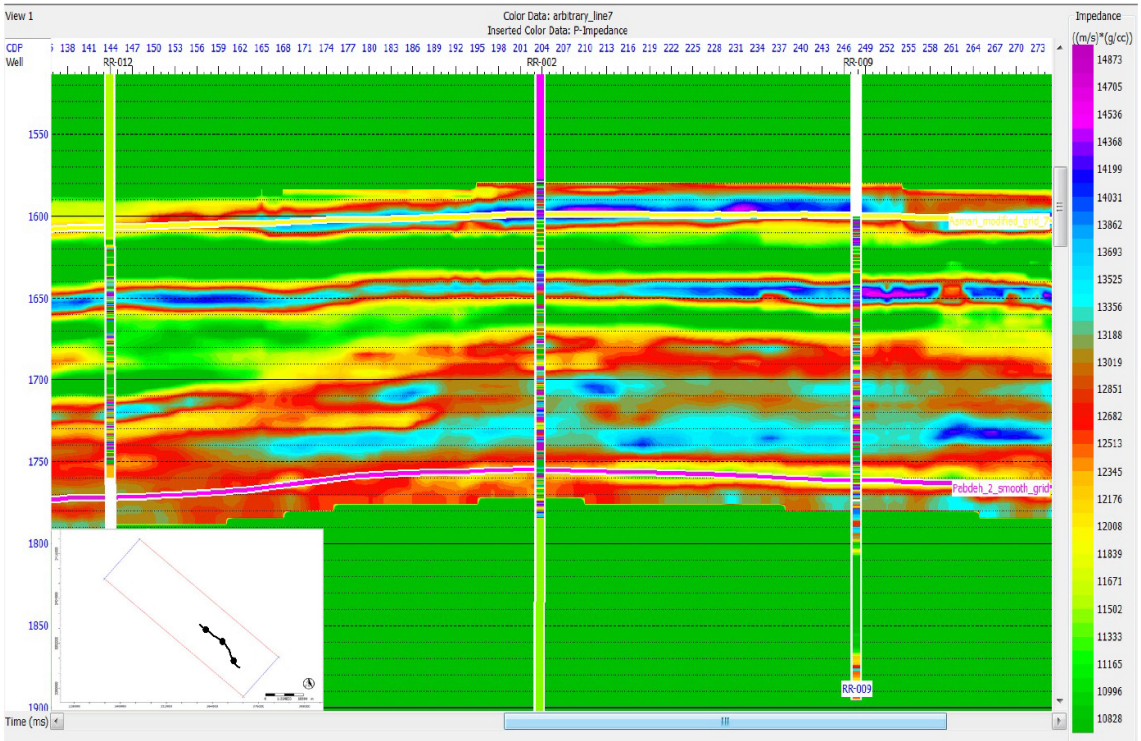

Figure 8. An arbitrary line from model based inversion cube passing through three well locations. The inserted color at the well locations represents acoustic impedance

Table 2. Multi-attribute list from a stepwise regression for prediction of effective porosity and water saturation in the Asmari reservoir of the Ramshir field

	Target	Final Attribute	Training Error	Validation Error
1	Porosity	Log (Inversion Result)	0.0324	0.0333
2	Porosity	Time	0.0311	0.0323
3	Porosity	Amplitude Weighted Cosine Phase	0.0300	0.0315
4	Porosity	X-Coordinate	0.0293	0.0308
5	Porosity	Filter 25/30-35/40	0.0286	0.0305
6	Porosity	Instantaneous Phase	0.0278	0.0299
1	Water Saturation	Dominant Frequency	0.1719	0.2293
2	Water Saturation	Amplitude Envelope	0.1453	0.2241
3	Water Saturation	Amplitude Weighted Frequency	0.1363	0.1737
4	Water Saturation	Derivative Instantaneous Amplitude	0.1320	0.1628

Using the other attributes in addition to acoustic impedance has shown that the single attribute regression is not a suitable method for prediction. To improve the prediction power, we need to use a group of attributes, simultaneously. The results of multi–regression analyses, for predicting water saturation and porosity, are displayed in Table 3. According to Table 3, adding more attributes will improve the prediction. This does not always mean that the added attributes are predicting the true signal in the target log. The validation error can be considered as a criterion for determining when to stop adding attributes to the input set (Russell, 2004).

According to Table 2, the six attributes for predicting porosity have been proposed. They include log (inversion result), time, amplitude weighted cosine phase, x–coordinate, filter 25/30–35/40 and instantaneous phase. Performing a similar process, the four attributes of dominant frequency, amplitude envelope, amplitude weighted frequency and derivative. Instantaneous amplitude could be considered as the optimal inputs for estimating water saturation. The relationships between the input seismic attributes and porosity and SW are shown in the cross plots of Fig. 9. Validation test is commonly used as a criterion to stop adding additional attributes when an optimal number of attributes is found. This process contained several stages that continue until in all wells the target log is estimated. In each stage, the squared error between the predicted and the actual log value is calculated. The process is repeated for the best two attributes, three attributes, and so on.

Table 3. Summary of effective porosity and water saturation prediction by single and multi-attribute regression analysis, and neural network for the studied field.

Target log	Method	Validation result		Quality check(application result)	
		Cross correlation	Average Error	Cross correlation	Average Error
Effective Porosity	Single attribute regression	0.582	0.053	0.612	0.052
	Multiple attribute regression	0.781	0.045	0.793	0.041
	Neural network (PNN)	0.931	0.042	0.954	0.033
Water Saturation	Single attribute regression	0.542	0.169	0.564	0.163
	Multiple attribute regression	0.692	0.139	0.718	0.122
	Neural network (PNN)	0.901	0.119	0.948	0.061

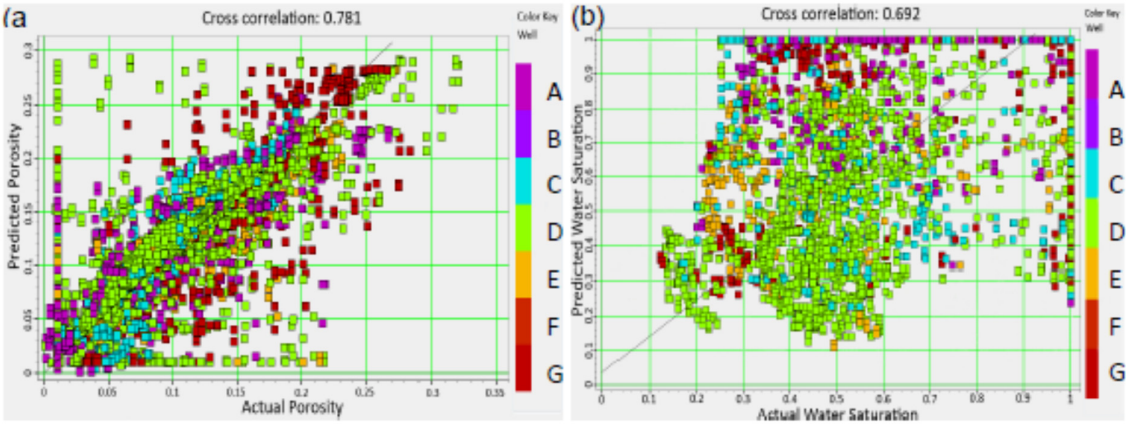

Figure 9. (a) Cross plot of actual and predicted effective porosity using multi attribute regression with correlation coefficient of 0.78. Color legend represents dataset from different wells used in this study. (b) Cross plot of actual and predicted water saturation (SW) with correlation coefficient of 0.69

Then, based on a plot of validation error versus the number of attributes, suitable attributes for prediction are identified as shown in Fig. 10, and also based on the results presented in Table 2, validation error after adding six attribute increases. This means the first six attributes are the optimal inputs for estimation of porosity and also four attributes are optimum for water saturation prediction.

Derived cross–plot of target log and different seismic attributes show dominant frequency attribute has the highest correlation with water saturation and, acoustic impedance has the lowest degree of error and the highest degree of correlation related to effective porosity. In some cases this single attribute transform produces good results, it does not mean a realistic value for target log, for example, acoustic impedance and dominant frequency are not the only seismic attribute which can be used to derive the petrophysical properties of the reservoir rocks in fact combinations of many attributes is needed to reservoir assessment. Thus, multi–linear regression and PNN neural network are used to predict the effective porosity and water saturation more precisely in the studied Formation.

Application of neural network for reservoir property estimation

The artificial neural network is a procedure or analysis method, especially when it becomes necessary to extract nonlinear and complex rules and relations governing a set of inputs data and the target property (Leiphart & Hart, 2001; Hampson et al., 2001; Walls et al., 2002; Pramanik et al., 2004; Calderon & Castagna, 2007; Gogoi & Chatterjee, 2019). In this paper, we used the Probabilistic Neural Network (PNN) to predict porosity and water saturation from seismic data. According to the results using the PNN algorithm gives less validation error.

Probabilistic Neural Network (PNN)

The PNNs approach includes computing weights which are based on the concept of distance in attribute space. The distance is calculated from a known point in space to an unknown point. PNN uses one or more measured values (independent variables) or derived parameters to predict the value of a single dependent variable (Specht, 1990; Masters, 1995). The Probabilistic neural network is a feed–forward neural network including input, hidden and output layer. As input for designing a PNN model, a sample set obtained from the well logs is split into training, validation and test subsets.

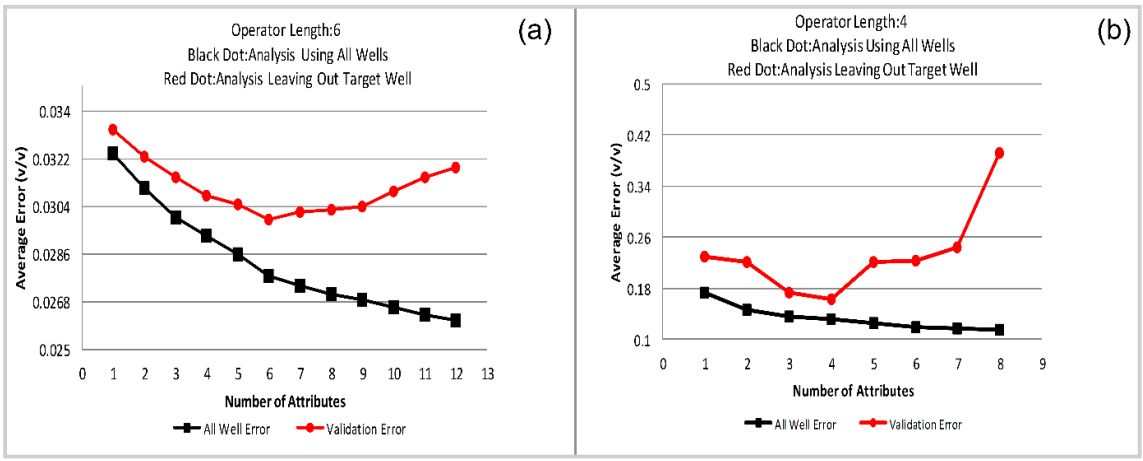

Figure 10. The graph showing average error versus the number of attributes to determine the optimal number of attributes to use in porosity (a) and water saturation (b) prediction, the Ramshir field. The optimal number of attributes to predict porosity and water saturation are six and four, respectively. The black curve indicates the error using all wells and the red curve shows the error plot when a well is removed from training set

The training process is carried out until at least one of the following conditions is met (i) a minimization of a mean square error (MSE) goal is achieved; (ii) occurrence of three consecutive epochs no improvements occur in the MSE for the validation subset; or (iii) a maximum number of iterations is completed. The test subset is used only to estimate the prediction power of the PNN by performing a blind test and it is not used for building the NN model (Leiphart & Hart, 2001). The PNN is considering as one of the most useful neural networks to estimate the petrophysical characteristics of seismic attributes by various researchers (Specht, 1990; Masters, 1995; Hampson et al., 2001; Pramanik et al., 2004; Kadkhodaie et al., 2009, Li, 2014). We compare three methods for predicting effective porosity and water saturation from seismic data. The data consist of a suite of well logs and a full stack 3D seismic survey from the Ramshir Field in Dezful Embayment. The 3D seismic is transformed into a number of attribute volumes. The attributes are combined in a nonlinear manner, via an Artificial Neural Network (ANN), or in a linear manner, via multilinear regression analysis, in order to predict the target porosity and water saturation from the available suite of field data. In this study we used neural networks as fallows:

At first, suitable attributes were selected by using the stepwise regression and its validation. Afterward, the statistical relationship between seismic attributes and target logs was obtained by neural network training in the well locations to derive a 3D porosity volume. As is seen in Fig. 11, porosity in the upper part is higher than the lower part especially in zone 1 and 2 which are shown with azure color. Green color indicates the low value and violet color shows a high value of porosity.

Porosity logs are entered at the well locations to compare the actual porosity with the predicted porosity. Map of an arbitrary line from the studied seismic cube is shown at the lower left of figure11. The PNN was trained by using the attributes extracted from multi–linear regression for effective porosity and water saturation estimation. After training, the network results show the correlation coefficient of 0.93 and 0.90 between actual and predicted for porosity and water saturation outperforming multi–linear regression (Table 3). As previously discussed, the result of validation is the criterion for the measure of network performance. Accordingly, for effective porosity neural network provided a higher correlation coefficient (0.93) and a lower average error (0.042), compared with multilinear regression. Fig12.

Overall, the neural network outperforms the regression model for estimation of porosity and water saturation in the Ramshir oilfield. As is seen in Fig.13, the arbitrary slices passing through the effective porosity cube correspond to high–porosity zones with a high volume of sand. The different horizon slices (Fig. 13) show that below the top of the Asmari (zone 2, Fig. 13b) represents the most effective porosity comparing to other zones. The same results were confirmed from inversion results (Fig. 11).

As aforementioned, the PNN can better establish the nonlinear relationships between seismic attributes, porosity and water saturation. Thus, in order to generate a water saturation volume, the neural network applied from the top to the base of the Asmari (Fig. 14).

As is seen, water saturation increases from zone 1 to zone 4. As shown in Figure.14b, zone 2 has a lower value of water saturation that is related to the presence of a productive oil–bearing zone. According to the results, water saturation in the central and northwestern parts of the reservoir is low that corresponds to the hydrocarbon–bearing area.

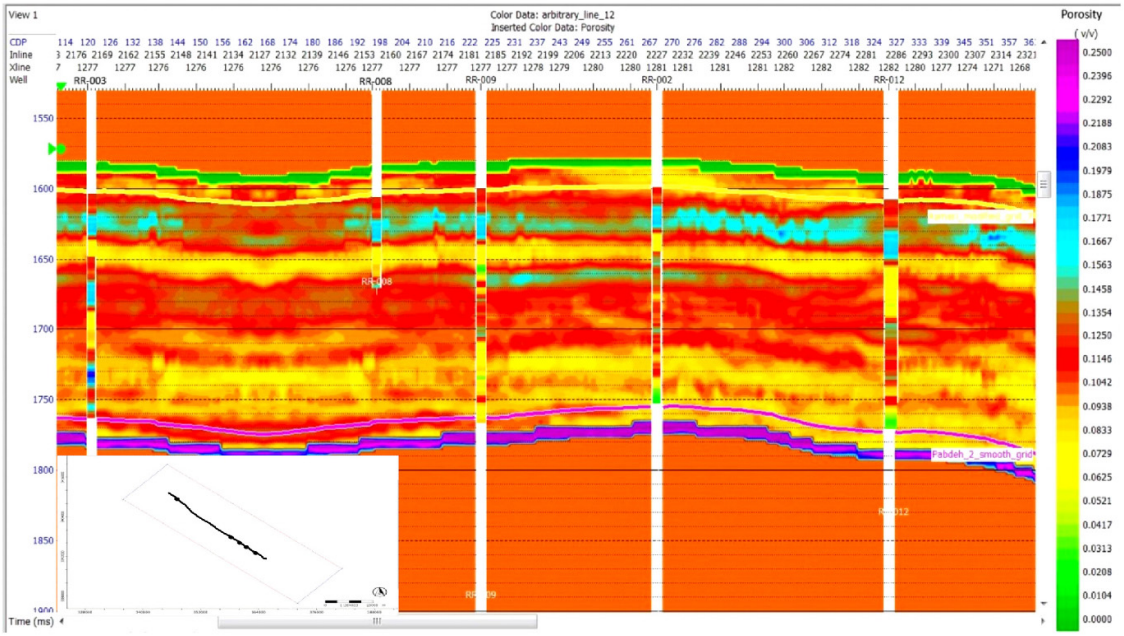

Figure11. Arbitrary line from porosity cube created using Probabilistic Neural Network method

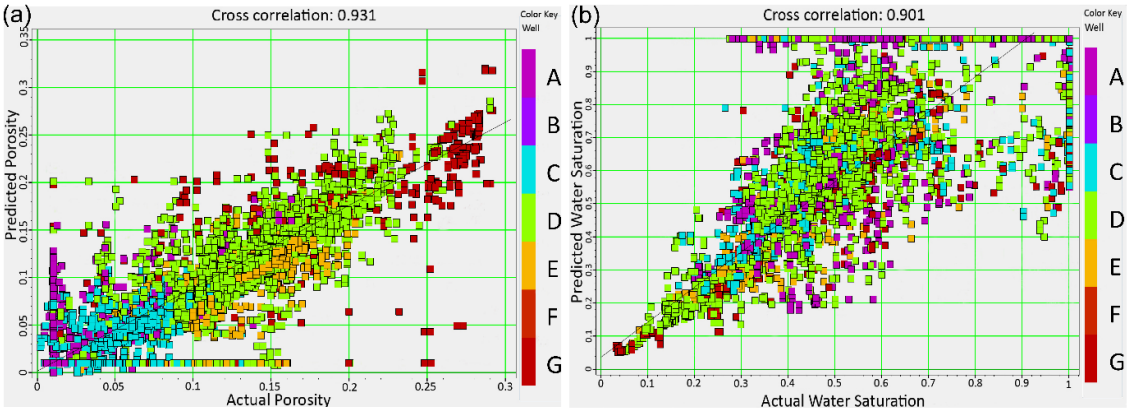

Figure 12. Crossplot of actual and predicted porosity (a) and water saturation (b) using neural network with correlation coefficient of 0.93 for porosity and 0.91 for water saturation. Color legend represents dataset from different wells used in this study

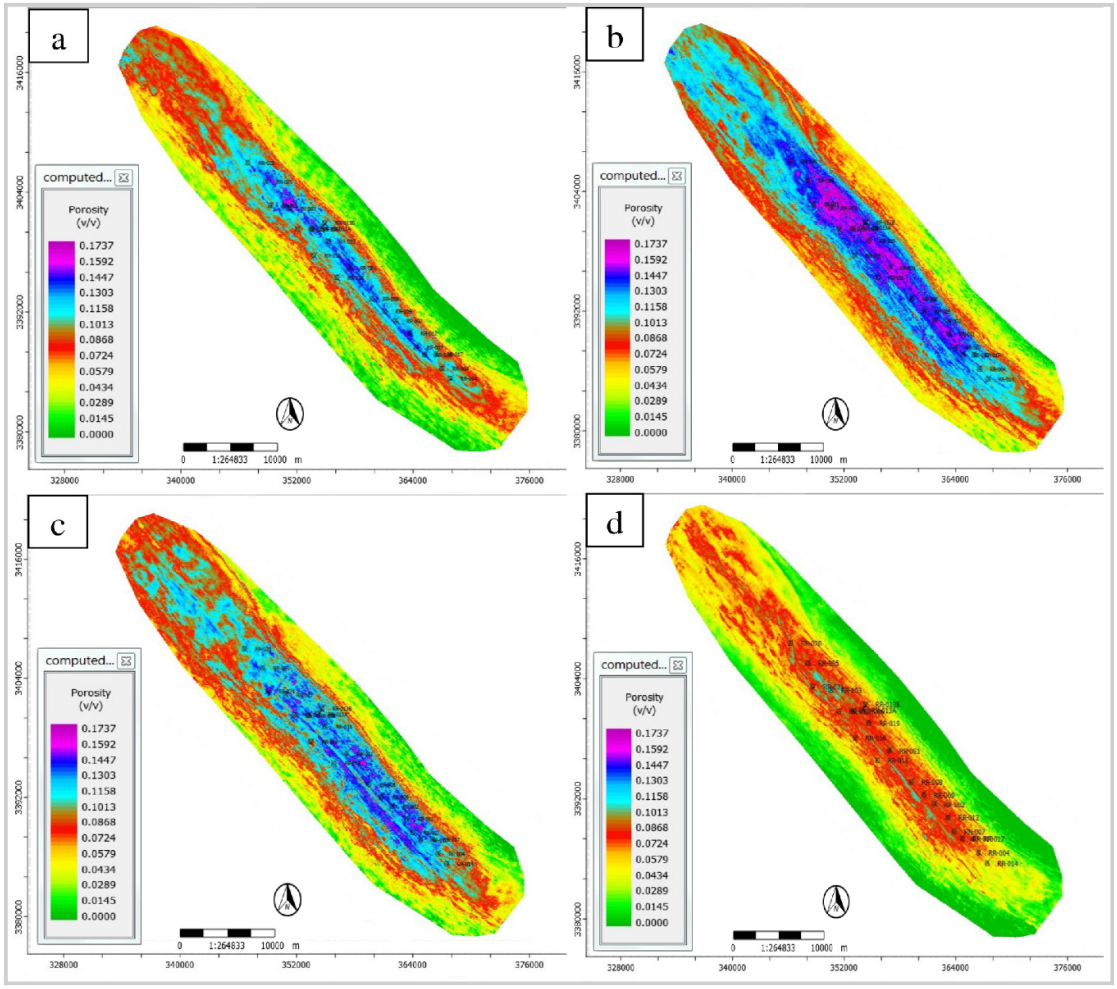

Figure 13. Different vertical slices of effective porosity maps of Asmari reservoir zones. a) 2 ms slice of Asmari Horizon(Z_1) , b) 2 ms slice of Asmari reservoir zone two (Z_2), c) 2 ms slice of Asmari reservoir zone three (Z_3), d) 2 ms slice of Asmari reservoir zone four (Z_4)

Geological reservoir characterization based on the acoustic impedance

In this study, for characterizing and classifying reservoir based on acoustic impedance variation, we used k–means clustering analysis. The results show a range from low to high values of the acoustic impedance over the Asmari reservoir. Accordingly, the Asmari reservoir can be classified into three main groups including low (AI <10500), medium (10510< AI < 12512) and high (AI >12550). Table 4 summarizes the main characteristics of each group. The study of core and thin sections of the Asmari reservoir indicates the difference in AI value between these clusters can be described based on the geological and petrophysical characteristics of the reservoir in the Ramshir field. They are described in each group as follows.

Cluster 1: includes more unconsolidated fine to medium grained, well sorted and rounded sandstones (Fig. 15). Based on evidence from core descriptions and thin sections study, they are mainly loose (free quartz grains) and slightly cemented with high amounts of hydrocarbon staining.

Cluster 2: based on acoustic impedance a large portion of reservoir facies are classified in this group. A variety of textures in mudstone and packstone/grainstone with dolomitic cement

are presence in this group. Vuggy, interparticle, and fracture are all the dominated pore types. Dissolution and dolomitization are also common in this group (Fig. 16).

Cluster 3: compared with the two previous groups, has high acoustic impedance and a low average effective porosity. Lithologically, this group consists of argillaceous limestone with mudstone and wackestone texture. Compaction features observed as solution seams and stylolites on core intervals and thin sections (Fig. 17)

Table 4. Asmari facies characteristic in differentiated clusters based on acoustic impedance (AI)

Asmari reservoir facies based on acoustic impedance (AI)		AI	PHIE	GR	Description
Low-AI facies Cluster 1	min	8210	0	5.9	unconsolidated fine to medium grained, well sorted and rounded sandstones, mainly loose, slightly cemented and has high value of hydrocarbon staining
	mean	9726	14	38	
	max	10510	17.3	75	
Medium-AI facies Cluster 2	min	10510	0	3.6	Dolomitic Bioclastic peloidal packstone/ grainstone with vuggy, interparticle and biomoldic porosity
	mean	11451	10	41	
	max	12510	16	83	
High-AI facies Cluster 3	min	12510	0	25	Argillaceous limestone with mudstone and wackestone texture and compaction features
	mean	13200	5	55	
	max	14581	11	126	

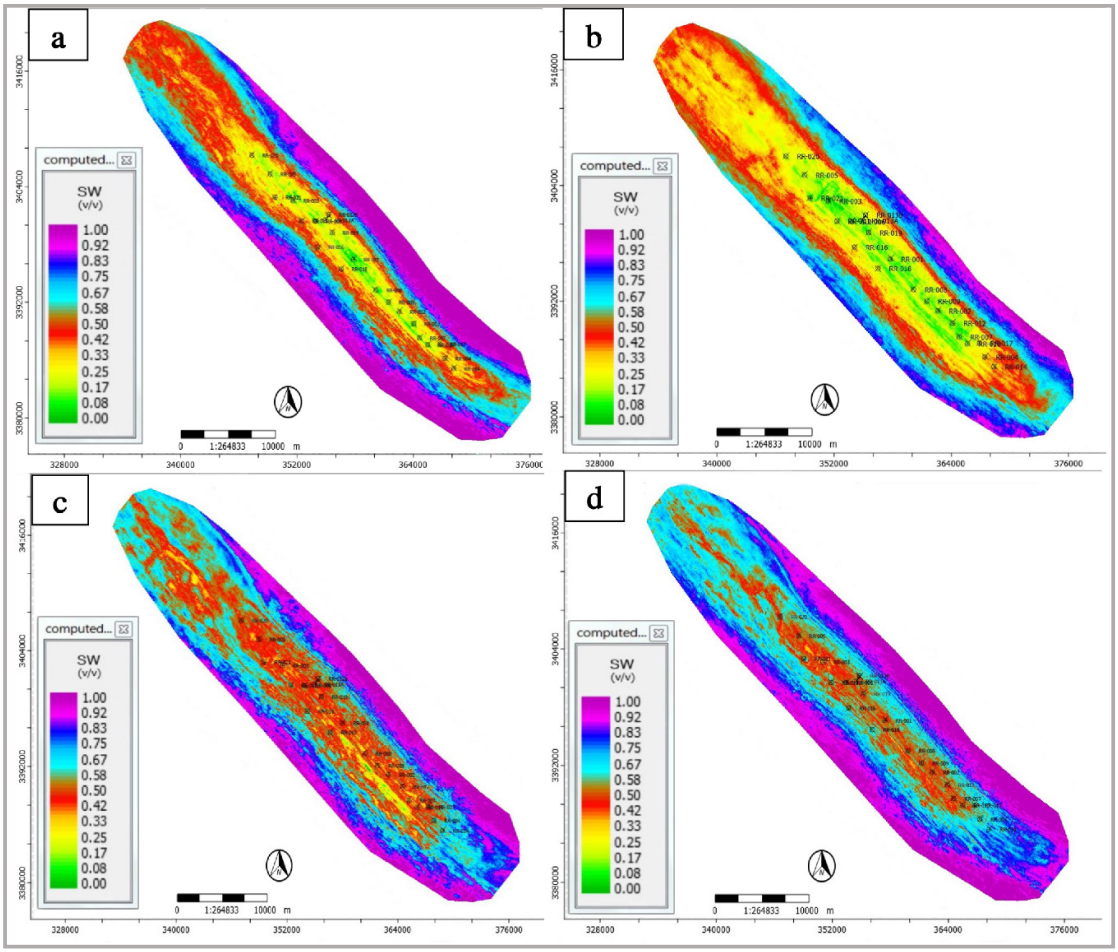

Figure 14. Different vertical slices of water saturation maps of Asmari reservoir production zones. a) 2 ms slice of Asmari Horizon (Z_1), b) 2 ms slice of Asmari reservoir zone two (Z_2), c) 2 ms slice of Asmari reservoir zone three (Z_3), d) 2 ms slice of Asmari reservoir zone four (Z_4)

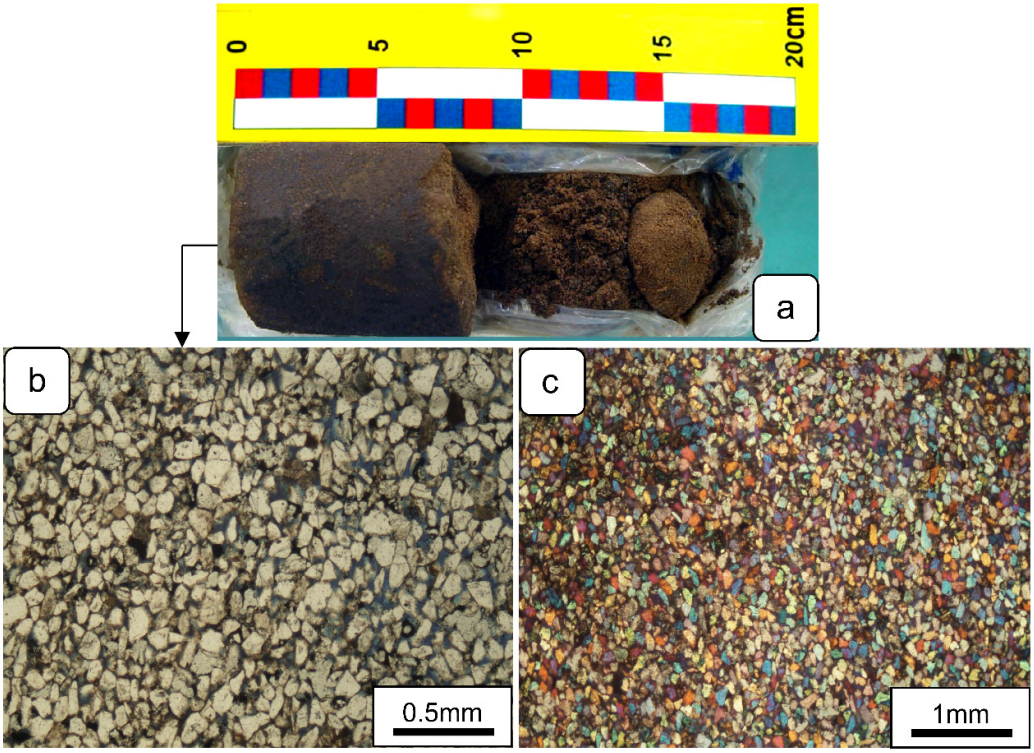

Figure 15. Core image and photomicrographs of cluster 1 from the Asmari reservoir, Ramshir field. a) Highly oil-stained loose sandstone (depth 2867.3 m). b, c) Well sorted and rounded free quartz grains(depth b 2867.3 m and depth c 2834.1m).

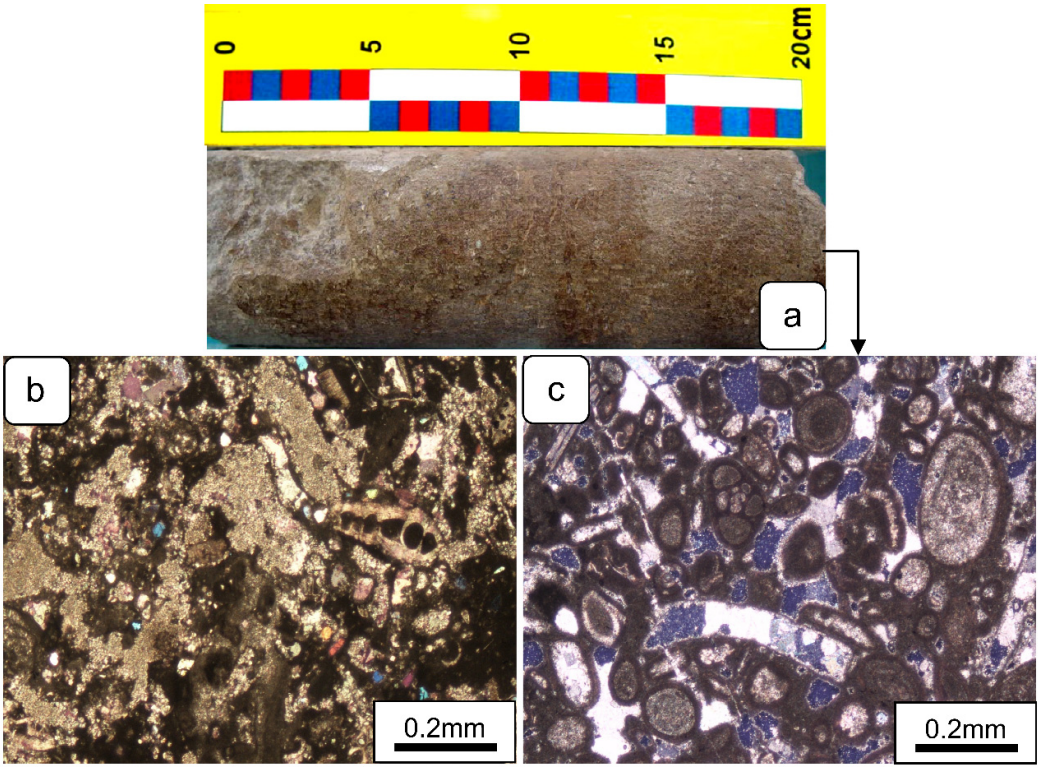

Figure16. Core image and photomicrographs of cluster 2. a) Brown limestone stained with hydrocarbon (depth 3005.5 m). b) Dolomitization in packstone (depth 2785.25 m). c) Vuggy porosities in ooid-bioclast grainstone (depth 3005.5 m).

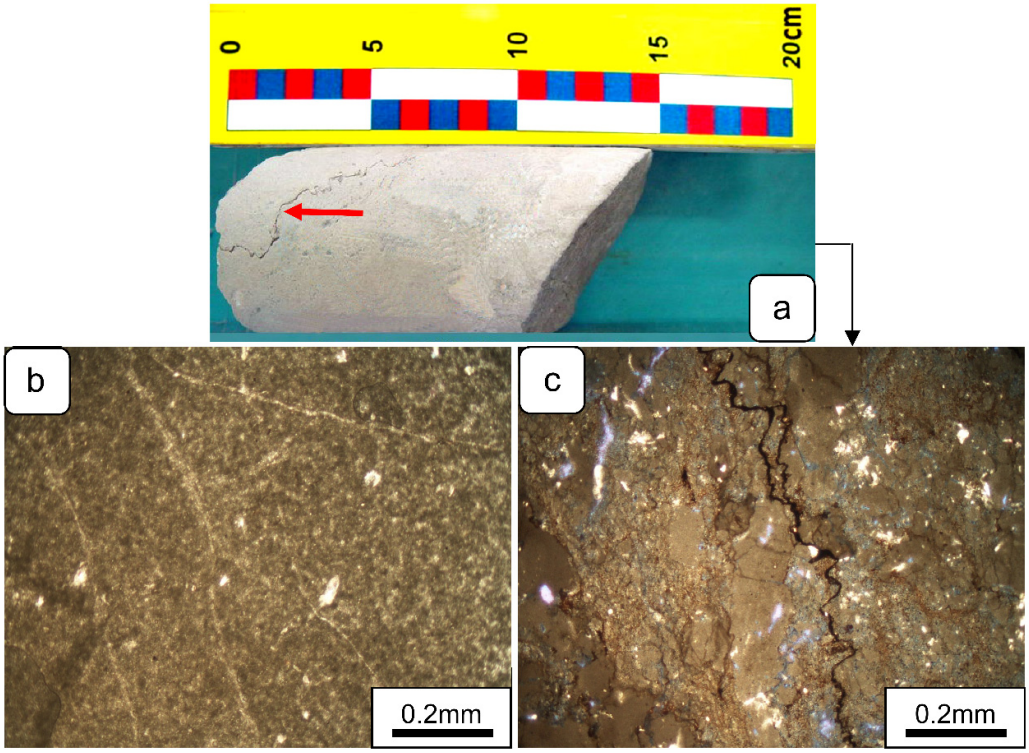

Figure 17. Core image and photomicrographs of cluster 3. a) Cream limestone with stylolites and solution seams (arrows) (depth 2803 m).b, c) mudstone with chemical compaction features are observed as solution seams and stylolites (depth b 2968.4 m and depth c 2803 m).

Results and discussion

In this study statistical methods have been applied based on both linear and non–linear algorithms on 3D seismic attributes and log data of the Ramshir oilfield. The analyzed dataset consists of 24 wells with measured porosity logs, along with the seismic volume and inverted results from the model based inversion methods.

The multi–attribute analysis as a suitable method was used for predicting effective porosity and water saturation. Step–wise multi–regression analysis and cross–validation tests were used to determine the optimal set of attributes. The multi–regression analysis is used to find a linear relationship between the seismic attributes and the measured reservoir property at the well locations. A non–linear relationship is also derived using neural networks. Cross–validation tests show the various levels of confidence in the prediction process. The probabilistic neural networks showed the lowest validation error, i.e. provided better results (Fig. 12). Based on the results of this study, neural network (PNN) can successfully predict reservoir porosity from the use of seismic attributes including acoustic impedance, Log (Inversion Result), Time, Amplitude Weighted Cosine Phase, X–Coordinate Filter 25/30–35/40 and Instantaneous Phase attributes. In order to predict water saturation, Dominant frequency, Amplitude Envelope, Amplitude Weighted Frequency and Derivative Instantaneous Amplitude used as the optimal inputs to predict water saturation based on neural network (PNN) (Table 2). The seismic inversion results demonstrated that the siliciclastics are more developed in the upper zones (especially zone 2) of the reservoir and decrease towards the lower zones. Accordingly, siliciclastics increase towards the west and the north of the field (Shadegan and Ahvaz fields) (Figs. 11 & 14). Based on core and thin sections study, variations in impedance data is related to the depositional, diagenetic and petrophysical characteristics of the Asmari reservoir rock. Hence, impedance data can be used to recognize the lateral and vertical variations in lithology

and facies. The inversion results show that low impedance in the upper part of the reservoir (green color) are mainly due to the sandstones lithologies. The low impedance in sandstone intervals is clearly related to sand and sandstone in zone 2. Besides this, porous grainstone, mudstone, wackestone, and boundstone with dolomitic cement exist showing medium acoustic impedance. The high acoustic impedance values (violet color) correspond to the consolidated and low porous mudstone/wackestone facies in the studied reservoir (Fig. 8). Hence, acoustic impedance served as a useful tool for identifying lithology and reservoir properties in the reservoir intervals.

Conclusion

In this study, integration of petrophysical interpretation and model based inverted acoustic impedance resulted in an effective estimation of reservoir properties in the Ramshir oilfield. For this purpose, model based inversion was used as an effective approach to obtain acoustic impedance attribute. Acoustic impedance inversion allowed a better understanding of the heterogeneities throughout the Asmari reservoir. 3D seismic data were used to investigate the lateral and vertical variations of effective porosity and water saturation in the studied reservoir. Such variations were described based on the geological characteristics of reservoir rock units. Base on the result of the core and thin section study, variations in acoustic impedance were related to geological and petrophysical characteristics of the Asmari reservoir. The high values of acoustic impedance are related to low porosity facies such as mudstones and argillaceous limestones, while low values of AI are in relation to sandstones. The moderate values of AI correspond to packstone/grainstone with vuggy and interparticle porosities. The correlation coefficient between the predicted and actual porosity and water saturation by using multiple regression analysis reaches 0.78 and 0.69, respectively. The probabilistic neural network improves the correlations to 0.93 and 0.90, respectively. The results suggest that the combination of post stack seismic inversion and PNN can effectively be applied to estimate reservoir properties. High effective porosity and hydrocarbon saturation values correspond to the west of the main producing unit. This can help to reduce the risks and costs of the exploration and master development plans.

Acknowledgments

The authors thank the Geology Department and Vice President for Research & Technology of the Ferdowsi University of Mashhad for their support (grant No. 3/38105). We acknowledge the National Iranian South Oil Company (NISOC) for sponsoring, providing the data and permission to publish the results of this research.

References

Abreu, V., Sullivan, M., Pirmez, C., Mohrig, D., 2003. Lateral accretion packages (LAPs): an important reservoir element in deep water sinuous channels. Marine and Petroleum Geology, 20: 631- 648.

Aleardi, M., 2018. Applying a probabilistic seismic-petrophysical inversion and two different rock physics models for reservoir characterization in offshore Nile delta. Geophysics, 148: 272-286.

Bosch, M., Mukerji, T., Gonzalez, E.F., 2010. Seismic inversion for reservoir properties combining statistical rock physics and geostatistics: A review. Geophysics, 75: 165-176.

Calderon, J.E., Castagna, J., 2007. Porosity and lithologic estimation using rock physics and multi-attribute transforms in Balcon Field, Colombia. The Leading Edge, 26: 142-150.

Chen, Q., Sidney, S., 1997. Seismic attribute technology for reservoir forecasting and monitoring. The Leading Edge, 16: 445-456.

Chopra, S., Marfurt, K. J., 2007. Seismic Attributes for Prospect Identification and Reservoir

Characterization: Geophysical Development Series 11, Society of Exploration Geophysics, 481 p.
Cooke, D., Schneider, W.A., 1983. Generalized linear inversion of reflection seismic data. Geophysics, 48: 665-676.
Cooke, D., Cant, J., 2010. Model-based Seismic Inversion: Comparing deterministic and probabilistic approaches. Canadian Society of Exploration. Geophysicists, CSEG Recorder, 35: 28-39.
Faraji, M. A., Kadkhodaie, A., Rezaee, R., Wood, D. A., 2017. Integration of core data, well logs and seismic attributes for identification of the low reservoir quality units with unswept gas in the carbonate rocks of the world's largest gas field. Journal of Earth Science, 28: 857-866.
Farfour, M., Yoon, W.J., Kim, J., 2015. Seismic attributes and acoustic impedance inversion in interpretation of complex hydrocarbon reservoirs. Journal of Applied Geophysics, 114: 68-80.
Gogoi, T., Chatterjee, R., 2019. Estimation of petrophysical parameters using seismic inversion and neural network modeling in upper Assam Basin, India, Geoscience Frontiers, 10(3):1113-1124.
Hampson, D.P., Schuelke, J.S., Quirein, J.A., 2001. Use of multiattribute transforms to predict log properties from seismic data. Geophysics, 66:220-236.
Haris, A., Pradana, G. S., Riyanto, A., 2017.Combination of Seismic Inversion and Spectral Decomposition to Identify Reservoir and Gas Content: A Case Study of CH Field, East Java Basin AIP Conference Proceedings 1862, 030163.
Huuse, M., Feary, D.A., 2005. Seismic inversion for acoustic impedance and porosity of Cenozoic cool-water carbonates on the upper continental slope of the Great Australian Bight. Marine Geology, 215:123-134.
Iturrarán-Viveros, U., Parra, J.O., 2014. Artificial Neural Networks applied to estimate permeability, porosity and intrinsic attenuation using seismic attributes and well log data. Journal of Applied Geophysics, 107:45-54.
John, A., Lake, L.W., Torres-Verdin, C., Srinivasan, 2005. Seismic Facies Identification and classification using simple statistics. Society of Petroleum Engineers. SPE 96577.
Kadkhodaie-Ilkhchi, A., Rezaee, M.R., Rahimpour-Bonab, H., Chehrazi, A., 2009. Petrophysical data prediction from seismic attributes using committee fuzzy inference system. Computers & Geosciences, 35: 2314-2330.
Kadkhodaie-Ilkhchi, R., Moussavi-Harami, R., Rezaee, R., Nabi-Bidhendi, M., Kadkhodaie Ilkhchi, A., 2014. Seismic inversion and attributes analysis for porosity evaluation of the tight gas sandstones of the Whicher Range field in the Perth Basin, Western Australia. Journal of Natural Gas Science and Engineering, 21: 1073-1083.
Kadkhodaie-Ilkhchi, R., Rezaee, R., Moussavi-Harami, R., Kadkhodaie-Ilkhchi, A., 2013. Analysis of the reservoir electrofacies in the framework of hydraulic flow units in the Whicher Range Field, Perth Basin, Western Australia. Journal of Petroleum Science and Engineering, 111: 106-120.
Khoshdel, H., Riahi, M.A., 2007. 3D porosity estimation using multi attribute analysis methods in one of the Persian Gulf oil fields. EUROPEC /EAGE Annual Conference and Exhibition, London, June 11-14: 1-12.
Khoshdel, H., Riahi, M.A., 2011. Multi attribute transform and neural network in porosity estimation of an offshore oil field. A case study. Journal of Petroleum Science and Engineering, 78:740-747.
Kumar, R., Das, B., Chatterjee, R., Sain, K., 2016. A methodology of porosity estimation from inversion of post stack seismic data. Journal of Natural Gas Science and Engineering, 28: 356-364.
Lavergne, M., Willm, C., 1977. Inversion of seismograms and pseudo velocity logs. Geophysical Prospecting, 25: 231-250.
Leiphart, D.J., Hart, B.S., 2001. Comparison of linear regression and a probabilistic neural network to predict porosity from 3D seismic attributes in Lower Brushy Canyon channeled sandstones, southeast New Mexico. Geophysics, 66: 1349-1358.
Leite, E.P., Vidal, A.C., 2011. 3D porosity prediction from seismic inversion and neural networks. Computers & Geosciences, 37: 1174-1180.
Li, M., 2014. Geophysical Exploration Technology: Applications in Lithological and Stratigraphic Reservoirs (1rd edition). Elsevier Inc.MA. USA.480 p.
Lindseth, R.O., 1979. Synthetic sonic logs: a process for stratigraphic interpretation. Geophysics, 44: 3-26
Mallick, S., 1995. Model based inversion of amplitude variations with offset data using a genetic algorithm. Geophysics, 60: 939-954.

Maurya, S.P., Singh, K.H., 2019. Predicting Porosity by Multivariate Regression and Probabilistic Neural Network using Model based and Coloured Inversion as External Attributes: A Quantitative Comparison. Journal of Geological Society of India, 93: 207-212.

Naeem, M., El-Araby, H.M., Khalil, M.K., Jafri, M.K., Khan, F., 2015. Integrated study of seismic and well data for porosity estimation using multi attribute transforms: a case study of Boonsville Field, Fort Worth Basin, Texas, USA. Arabian Journal of Geoscience, 8: 8777-8793.

Na'imi, S.R., Shadizadeh, S.R., Riahi, M.A., Mirzakhanian, M., 2014. Estimation of reservoir porosity and water saturation based on seismic attributes using support vector regression approach. Journal of Applied Geophysics, 107: 93-101.

NISOC, 2016. Map of distribution of oil and gas fields in the Zagros basin, IranNational .(50,000/1) ,Iranian South Oil Company.(unpublished).Ahwaz, Iran

Ogiesoba, O.C., 2010. Porosity prediction from seismic attributes of the Ordovician Trenton Black River groups, Rochester field, southern Ontario. American Association of Petroleum Geologists Bulletin, 94:1673-1693.

Osleger, D.A., Montanez, I.P., 1996. Cross-platform architecture of a sequence boundary in mixed siliciclastic-carbonate lithofacies, Middle Cambrian, southern Great Basin, USA. Sedimentology, 43: 197-217.

Perez-Muoz, T., Velasco-Hernandez, J., Hernandez-Martinez, E., 2013. Wavelet transform analysis for lithological characteristics identification in siliciclastic oil fields. Journal of Applied Geophysics, 98:298-308.

Pramanik, A.G., Singh, V., Vig, R., Srivastava, A.K., Tiwary, D.N., 2004. Estimation of effective porosity using geostatistics and multiattribute transforms: A case study. Geophysics, 69: 352-372.

Prospectiuni., S.A. & Pedex, 2009. Final report on 3D land seismic acquisition Ramshir area, National Iranian South Oil Company (NISOC), Iran.

Raeesi, M., Moradzadeh, A., Ardejani, F.D., Rahimi, M., 2012. Classification and identification of hydrocarbon reservoir lithofacies and their heterogeneity using seismic attributes, logs data, and artificial neural networks. Journal of Petroleum Science and Engineering, 82:151-165.

Rezaee, M.R., Slatt, R., Kadkhodaie, A., 2006. Application of Intelligent Systems for Generating Wireline Logs. Earth Science Journal, University of Oklahoma, USA, 2006 Edition. P.56-66.

Rezvandehy, M., Aghababaei, H., Tabatabaee Raissi, S.H., 2011. Integrating seismic attributes in the accurate modeling of geological structures and determining the storage of the gas reservoir in Gorgan Plain (North of Iran). Journal of Applied Geophysics, 73: 187-195.

Russell, B.H., 2004. The application of multivariate statistics and neural networks to the prediction of reservoir parameters using seismic attributes. Ph.D. Dissertation. University of Calgary, Alberta. 392p.

Russell, B., Hampson, D., 1991. A comparison of post stack seismic inversion methods: In 61st Annual international Meeting, Society of Exploration Geophysicists, Expanded abstracts, pp. 876-878.

Saltzer, R., Finn, C., Burtz, O., 2005. Predicting V shale and porosity using cascaded seismic and rock physics inversion. The Leading Edge, 24: 732-736.

Schlumberger, 2003. A geological overview of Iran. Reservoir optimization conference, 19 p.

Sepehr, M., Cosgrove, J.W., 2005. The Role of the Kazerun fault zones in the formation and deformation of the Zagros fold-thrust belt, Iran. Tectonics, 24: 1-13.

Schultz, P. S., Ronen, S., Hattori, M., Corbett, C., 1990a. Seismic guided estimation of log properties, part 1: The Leading Edge, 11: 543 - 514.

Schultz, P. S., Ronen, S., Hattori, M., Corbett, C., 1990b. Seismic guided estimation of log properties, part 2: The Leading Edge, 11: 670-678

Simm, R., Bacon, M., 2014. Seismic Amplitude: An interpreter's handbook (1rd edition). Cambridge University Press, 281 p.

Snedden, J.W., 2013. Channel-body basal scours: Observations from 3D seismic and importance for subsurface reservoir connectivity. Marine and Petroleum Geology, 39: 150-163.

Specht, D.F., 1990. Probabilistic neural networks. Neural networks, 3: 109-118.

Swisi A., 2009. Post-and pre-stack attribute analysis and inversion of Blackfoot 3D seismic dataset. M.Sc. thesis, Department of Geological Science, University of Saskatchewan.154p.

Tonn, R., 2002. Neural network seismic reservoir characterization in heavy oil reservoir. The Leading Edge, 21: 309-312.

Walls, J.D., Taner, M.T., Taylor, G., Smith, M., Carr, M., Derzhi, N., Drummond, J., McGuire, D., Morris, S., Bregar, J., 2002. Seismic reservoir characterization of a US Midcontinent fluvial system using rock physics, poststack seismic attributes, and neural networks. The Leading Edge, 21: 428-436.

Yao, T., Journel, A.G., 2000. Integrating seismic attribute maps and well logs for porosity modeling in a west Texas carbonate reservoir: addressing the scale and precision problem. Journal of Petroleum Science and Engineering, 28: 65-79.